6 Frictional Contact Problems

In this chapter, we apply our monotone multigrid method to contact problems involving Coulomb friction. We present two algorithms for solving frictional contact problems. The first one is based on a fixed point iteration proposed in [Has83]. The second one is based on a Gauß–Seidel like update of the boundary stresses. Although up to now no convergence theory for this algorithm is available, our numerical experiments show the reliability. Moreover, using the Gauß–Seidel like method, no outer iteration was necessary at all. Thus, it is possible to solve solve nonlinear frictional contact problems with nearly the same computational amount as is required for *linear* problems.

Before describing both methods in detail, let us shortly discuss the difficulties arising when solving frictional contact problems. The first difficulty is that the functional associated with Signorini's problem with Coulomb friction is nonconvex, nonquadratic and nondifferentiable. Thus, standard existence and uniqueness results from convex analysis cannot be applied. Nevertheless, for sufficiently small coefficients of friction, the solution to Signorini's problem with Coulomb friction has been shown to exists, see [Eck96, NJH80, NJH80] and the monograph [HHNL88]. Unfortunately, the existence proof given in [NJH80] cannot be used directly to derive a numerical method, since it involves Tychonov's fixed point theorem. In [Eck96], a penalty approach is used for proving existence and regularity of the solution. Therefrom, a numerical penalty method can be derived. Since regularization leads to additional errors of the discrete solution, we do not follow this approach. Rather, we try to resolve the nondifferentiability directly, which is possible by using monotone multigrid methods.

For the numerical solution of contact problems with Coulomb friction we follow [Jar83] and use a fixed point iteration in the normal stresses. Then, in every iteration step we have to solve a contact problem with so called *Tresca* friction, i.e., a reduced frictional problem with prescribed normal stresses. Since this kind of problem turns out to be convex, we can apply a suitable modification of our monotone multigrid as an *inner solver* within the fixed point iteration. The resulting algorithm is an reliable tool for solving contact problems involving Coulomb friction. To avoid the outer iteration, we also introduce a Gauß–Seidel like variant of the fixed point iteration. This variant shows to be as reliable as the fixed point iteration but is significantly faster. Unfortunately, the resulting algorithm is based on the minimization of a nonconvex functional and so far no convergence theory is available.

The remainder of this chapter is structured as follows: In Section 6.2, we give the weak formulation of Signorini's problem with Coulomb friction and give an existence result. In Section 6.2, we present the discrete fixed point iteration. Moreover, we explain the necessary modifications of the monotone multigrid method for the resulting piecewise smooth obstacle problem, which are based on [Kor01]. Finally, in Section 6.3, we give numerical results illustrating the accuracy and efficiency of the resulting method in two and three space dimensions.

For the case of elastic contact with Coulomb friction, we refer the reader to Section 7.

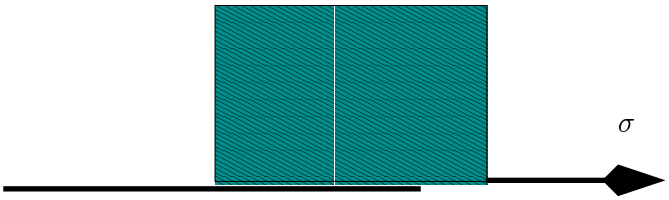

Figure 6.1: Simple onedimensional frictional device

6.1 Weak Formulation

In this section, we present the variational formulation of Signorini's problem with friction. We give a motivation for Coulomb's law of friction and give the weak formulation of Signorini's problem with friction. The resulting weak formulation is exploited in Section 6.3, when we derive our monotone multigrid method for frictional problems.

To motivate the ideas, let us start with a simple onedimensional frictional device as depicted in Figure 6.1. From experiments, the following behavior of this simple device is known:

1. The absolute value of the frictional stress σ in the device cannot be greater than some maximal stress $\sigma_{\max}$.

2. If the absolute value of the frictional stress reaches the maximal stress $\sigma_{\max}$, then sliding *opposite* to σ occurs. That is, the device tries to compensate the frictional stress by a displacement in opposite direction.

In other words, defining the set $[-\sigma_{\max}, \sigma_{\max}]$ of admissible stresses, we have seen that $\sigma \in [-\sigma_{\max}, \sigma_{\max}]$. Moreover, if $|\sigma| = \sigma_{\max}$, then the frictional device responses by a displacement u opposite to σ, i.e., $u = -\lambda\sigma$ for some $\lambda \geq 0$. Now, we assume additionally that the critical stress $\sigma_{\max}$ is proportional to the normal stress σ_n. Then, we have derived *Coulomb's law of friction*

$$\begin{aligned} \boldsymbol{u}_T &= 0\,, \quad |\boldsymbol{\sigma}_T(u)| < \mathcal{F}|\sigma_n(u)| \\ \boldsymbol{u}_T &= -\lambda\boldsymbol{\sigma}_T(u)\,, \quad |\boldsymbol{\sigma}_T(u)| = \mathcal{F}|\sigma_n(u)|\,, \end{aligned} \tag{6.1}$$

with $\lambda \geq 0$. Here, we have $\boldsymbol{u} \in \mathbb{R}^d$ and $|\cdot|$ stands for the Euclidian vector norm in $\mathbb{R}^d$ or $\mathbb{R}^{d-1}$. $\mathcal{F} > 0$ is the *coefficient of friction*. Clearly, Coulomb's law of friction is a *local* friction law. The frictional response at a point x depends only on the stresses developed at x. From (6.1) we also see, that we can divide all points at the contact boundary into *sticking* points and *sliding* points. A point x is called sticky, if no tangential displacement occurs, i.e., if $\boldsymbol{u}_T(x) = 0$. It is called sliding, if $\boldsymbol{u}_T(x) \neq \boldsymbol{0}$. Figure 6.2 illustrates the relation between tangential stress and normal stress for a sliding and a sticky point. For existence results concerning different nonlinear friction laws, see. e.g., [MO87, RMOC86] and the references cited therein.

Remark 6.1 *Equations (6.1) can also be written in the form*

$$\begin{aligned} |\boldsymbol{\sigma}_T(u)| &< \mathcal{F}|\sigma_n(u)|\,, \quad (\mathcal{F}|\sigma_n(u)| - |\boldsymbol{\sigma}_T(u)|)\,\boldsymbol{u}_T = 0\,, \\ |\boldsymbol{\sigma}_T(u)| &\leq \mathcal{F}|\sigma_n(u)|\,, \quad \boldsymbol{\sigma}_T \cdot \boldsymbol{u}_T + \mathcal{F}|\sigma_n(u)|\,|\boldsymbol{u}_T| = 0 \end{aligned}$$

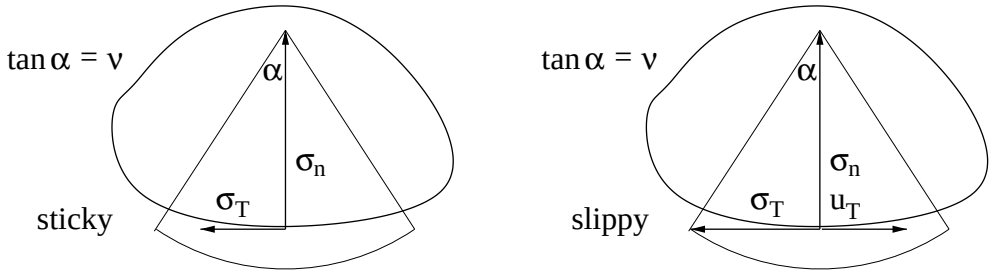

Figure 6.2: Sticky node (left) and sliding node (right)

Let us now combine Coulomb's law of friction with Signorini's problem in linear elasticity. By simply merging (6.1) and (2.1), we get the following boundary value problem in linear elasticity

$$\begin{aligned}
-\sigma_{ij}(\boldsymbol{u})_{,j} &= f_i\,, && \text{in } \mathscr{B}\,,\\
\boldsymbol{u} &= 0\,, && \text{on } \Gamma_D\,,\\
\sigma_{ij}(\boldsymbol{u})\cdot \boldsymbol{n}_j &= p_i\,, && \text{on } \Gamma_F\,,\\
\sigma_n(\boldsymbol{u}) = 0 \text{ and } \boldsymbol{\sigma}_T(u) &= 0\,, && \text{if } u_n < g \text{ on } \Gamma_S\,,\\
\sigma_n(\boldsymbol{u}) &< 0\,, && \text{if } u_n = g \text{ on } \Gamma_S\,,\\
\boldsymbol{u}_T &= 0\,, && \text{if } |\boldsymbol{\sigma}_T(u)| < \mathcal{F}|\sigma_n(u)|\,,\\
\boldsymbol{u}_T &= -\lambda\boldsymbol{\sigma}_T(u)\,, && \text{if } |\boldsymbol{\sigma}_T(u)| = \mathcal{F}|\sigma_n(u)|\,, \quad \lambda \geq 0
\end{aligned} \tag{6.2}$$

The stress tensor $\boldsymbol{\sigma}$ is given by (2.10). Problem (6.2) is called *Signorini's problem with Coulomb friction*. In addition to the assumptions on the data g, $\boldsymbol{f}$ and $\boldsymbol{p}$ made in Section 2.2, we assume for the coefficient of Friction $\mathcal{F} \in L^\infty(\Gamma_S)$ and $\mathcal{F} \geq \mathcal{F}_0 > 0$ almost everywhere on Γ_S.

We now derive a variational formulation of Problem (6.2). To this end, we introduce the nonlinear functional $\omega\colon \boldsymbol{H} \times \boldsymbol{H} \longrightarrow \mathbb{R}$ by

$$\omega(\boldsymbol{u},\boldsymbol{v}) = \int_{\Gamma_S} \mathcal{F}\,|\sigma_n(\boldsymbol{u})|\,|\boldsymbol{v}_T|\,da\,. \tag{6.3}$$

The functional ω characterizes the *virtual work of the frictional forces*. By means of the functional ω, we can rewrite Problem (6.2) as a variational inequality: Find $\boldsymbol{u} \in \mathcal{K}$

$$a(\boldsymbol{u},\boldsymbol{v}-\boldsymbol{u}) + \omega(\boldsymbol{u},\boldsymbol{v}) - \omega(\boldsymbol{u},\boldsymbol{u}) \;\geq\; f(\boldsymbol{v}-\boldsymbol{u})\,, \qquad \boldsymbol{v} \in \mathcal{K}\,. \tag{6.4}$$

This is done by integrating by parts and by exploiting the boundary conditions, see, e.g., the monographs [KO88, HHNL88]. The following theorem can be found in [DL72, HHNL88, KO88].

Theorem 6.2 *Any solution of (6.4) is a solution of (6.2). If $\boldsymbol{u}$ is a sufficiently smooth solution of (6.2), then also (6.4) holds.*

Unfortunately, the functional ω is nonconvex, nonquadratic and nondifferentiable. Thus, standard results from convex analysis cannot be applied to gain a solution of the variational inequality (6.4). For the case of an infinite strip in $\mathbb{R}^2$, the existence of the solution has been shown in [NJH80]. Here, also estimates of the solution with respect to the boundary data are given. In [Jar83], existence results are shown for more general domains. Using a penalty approach for the analysis, Eck showed in [Eck96], see also [EJ98], existence and regularity of the solution to both, the static and the dynamic problem of elastic contact with Coulomb friction. He also derived upper bounds $B_{\mathcal{F}}^{(2)}$ and $B_{\mathcal{F}}^{(3)}$ given by

$$\begin{aligned} B_{\mathcal{F}}^{(2)} &= \sqrt{1-\tfrac{1}{4}(\tfrac{1-2\nu}{1-\nu})^2}\,, \quad d=2 \\ B_{\mathcal{F}}^{(3)} &= \sqrt{1-\tfrac{1}{4(1-\nu)}}\,, \quad d=3\,, \end{aligned}$$

for the coefficient of friction $\mathcal{F}$ for two and threedimensional problems, respectively. For $\mathcal{F} < B_{\mathcal{F}}^{(3)}$, $i = 1, 2$, he was able to proof the existence of the solution to problem (6.2). In Figure 6.3, the bounds $B_{\mathcal{F}}^{(2)}$ and $B_{\mathcal{F}}^{(3)}$ are depicted.

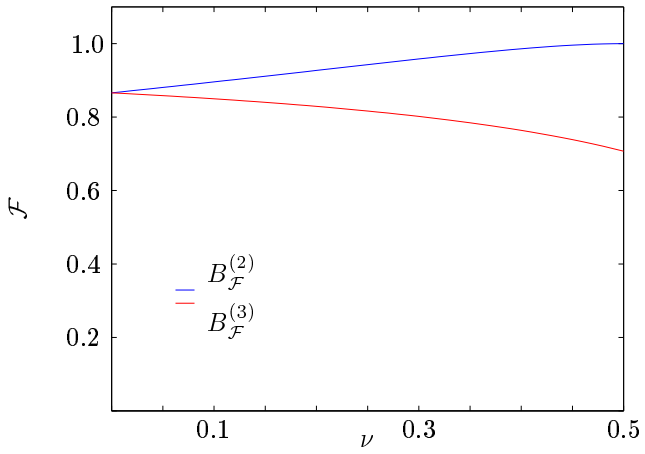

Figure 6.3: Bounds for the Friction coefficient $\mathcal{F}$ versus Poisson number ν

Remark 6.3 *Let us emphasize a remarkable feature of Signorini's problem with Coulomb friction. Although Problem (6.2) is considered as a "static" problem, it's solution is in general not the limit of a dynamic contact problem with friction. Rather, it should be interpreted as an incremental time step of a discretization of the dynamic problems using backward Euler scheme. For details, we refer the reader to [Eck96], Section (1.4).*

6.2 Fixed Point Iteration

In this section, we introduce the fixed point iteration used for solving problem (6.2). By means of this fixed point iteration, the nonconvex minimization problem (6.4) is trans-

formed into a sequence of convex minimization problems, i.e., a sequence of contact problems with Tresca friction. These convex minimization problems can be solved numerically using a suitable modification of our monotone multigrid method. Moreover, we present a new Gauß–Seidel like algorithm for solving contact problems involving Coulomb friction. In all of our numerical experiments, this algorithm converges faster than the fixed point iteration. Unfortunately, so far no convergence theory for this Gauß–Seidel like algorithm is available.

The fixed point iteration used to solve frictional contact problems has been introduced and analyzed in [Has83], see also the monograph [HHNL88]. To fix ideas, let us assume for the moment that the normal stress $\sigma_n \in H^{-1/2}(\Gamma_S)$ at the contact boundary is known. From the boundary conditions on Γ_S in (6.2) we know that $\sigma_n \leq 0$. To be more precise, we have $-\sigma_n \in H_+^{-1/2}(\Gamma_S)$, where $H_+^{-1/2}(\Gamma_S)$ is the convex cone of all nonnegative functionals over the Sobolev space $H^{1/2}(\Gamma_S)$. For $\sigma_n = \sigma_n(\boldsymbol{u})$, we can rewrite the functional of frictional work (6.3) in terms of the duality pairing $\langle \cdot, \cdot \rangle$ on $H^{-1/2}(\Gamma_S) \times H^{1/2}(\Gamma_S)$ as

$$\omega(\boldsymbol{u}, \boldsymbol{v}) = \langle \mathcal{F}|\sigma_n|, |\boldsymbol{v}_T| \rangle \,.$$

Following [Has83], we now consider for any fixed $\tau \in H_+^{-1/2}(\Gamma_S)$ the following problem: Find $\boldsymbol{u} = \boldsymbol{u}(\tau) \in \mathcal{K}$ such that

$$a(\boldsymbol{u}, \boldsymbol{v} - \boldsymbol{u}) + \langle \mathcal{F}|\tau|, |\boldsymbol{v}_T| - |\boldsymbol{u}_T| \rangle \;\geq\; f(\boldsymbol{v} - \boldsymbol{u}) \,, \qquad \boldsymbol{v} \in \mathcal{K} \,. \tag{6.5}$$

This gives motivation to define the following mapping

$$\Psi \colon H_+^{-1/2}(\Gamma_S) \longrightarrow H_+^{-1/2}(\Gamma_S) \,, \qquad \tau \mapsto \Psi(\tau) = -\sigma_n(\boldsymbol{u}(\tau)) \,, \tag{6.6}$$

where $\boldsymbol{u}$ is a solution of the problem (6.5) with reduced friction. Thus, a function $\boldsymbol{u}$ is said to be a *weak solution of the Signorini problem with Coulomb friction*, if it's negative boundary stress $-\sigma_n(\boldsymbol{u})$ is a fixed point of the mapping Ψ. The existence of a fixed point of $\boldsymbol{u}$ can be shown using Tychonov's fixed point theorem, provided the coefficient of Friction $\mathcal{F}$ is sufficiently small. For details, we refer to [NJH80, Jar83, HHNL88]. Here, let us only mention the following regularity result for problem (6.5):

Theorem 6.4 ([Has83]) *For any $\alpha \in (0, 1/4)$ and $\tau \in H_+^{-1/2+\alpha}(\Gamma_S)$, the corresponding $\sigma_n(\boldsymbol{u}(\tau)) \in H_-^{-1/2+\alpha}(\Gamma_S)$, or, equivalently, Ψ maps $H_+^{-1/2+\alpha}(\Gamma_S)$ into itself and*

$$\|\Psi(\tau)\|_{H^{-1/2+\alpha}(\Gamma_S)} \;\leq\; c_1 \|\tau\|_{H^{-1/2+\alpha}(\Gamma_S)} + c \|f\|_{\boldsymbol{L}^2(\mathscr{B})} \,,$$

where c is an absolute constant and $c_1 > 0$ depends on α and $\mathcal{F}$ in such a way that $c_1 \to 0+$ whenever $\max_{\Gamma_S} \mathcal{F} \to 0+$.

In what follows, for notational convenience we assume the coefficient of friction $\mathcal{F}$ to be constant. Before defining our *discrete* fixed point iteration, let us study the reduced frictional problem (6.5). Since the normal stress τ are assumed to be known, the functional of frictional work $\omega \colon \boldsymbol{H} \times \boldsymbol{H} \longrightarrow \mathbb{R}$ reduces to a functional

$$\omega \colon \boldsymbol{H} \longrightarrow \mathbb{R}, \qquad \omega(\boldsymbol{v}) = \int_{\Gamma_S} \mathcal{F}\tau |\boldsymbol{v}_T| \, da \,.$$

If necessary, we write ω_τ instead of ω. In consequence, the variational inequality (6.2) reduces to: Find $\boldsymbol{u} \in \mathcal{K}$

$$a(\boldsymbol{u}, \boldsymbol{v}-\boldsymbol{u}) + \omega_\tau(\boldsymbol{v}) - \omega_\tau(\boldsymbol{u}) \geq f(\boldsymbol{v}-\boldsymbol{u}), \qquad \boldsymbol{v} \in \mathcal{K}. \tag{6.7}$$

The function ω_τ is continuous on $\boldsymbol{H}$, convex and nondifferentiable. In particular, ω_τ is l.s.c. on $\boldsymbol{H}$ and thus subdifferentiable. Following [KO88, Theorem 10.2], there exist a unique solution of the variational inequality (6.7). This solution is characterized as the unique minimizer of the energy functional $\hat{\mathcal{J}}$ defined by

$$\hat{\mathcal{J}}(\boldsymbol{u}) = \mathcal{J}(\boldsymbol{u}) + \omega(\boldsymbol{u}) \tag{6.8}$$

on $\mathcal{K}$. We note that the uniqueness of the solution is a consequence of the strict convexity of $\hat{\mathcal{J}}$. There is also a strong formulation of the reduced variational inequality (6.7), see, e.g., [KO88, HHNL88]. For given $\tau > 0$, we have

$$\begin{aligned}
-\sigma_{ij}(\boldsymbol{u})_{,j} &= f_i\,, && \text{in } \mathscr{B}\,,\\
\boldsymbol{u} &= 0\,, && \text{on } \Gamma_D\,,\\
\sigma_{ij}(\boldsymbol{u})\cdot \boldsymbol{n}_j &= p_i\,, && \text{on } \Gamma_F\,,\\
\mathcal{F}|\sigma_n(\boldsymbol{u})| &= \tau && \text{on } \Gamma_S\,,\\
|\boldsymbol{\sigma}_T(\boldsymbol{u})| &< \tau && \text{then } \boldsymbol{u}_T = 0\,,\\
|\boldsymbol{\sigma}_T(\boldsymbol{u})| &= \tau && \text{then there exists } ,\lambda \geq 0 \text{ on } \Gamma_S\,,\\
& && \quad \text{such that } \boldsymbol{u}_T = -\lambda \boldsymbol{\sigma}_T\,.
\end{aligned}$$

Now, in order to derive a discrete variant of the fixed point iteration (6.6), we need to define suitable discrete normal stresses μ_n and a corresponding discrete space of boundary stresses, the *Lagrange multiplier space*. Our starting point is the definition of the discrete boundary stresses on the basis of Green's theorem, i.e., $\boldsymbol{\mu} \in \boldsymbol{M}^{(j)}$

$$\langle \boldsymbol{\mu}, \boldsymbol{v} \rangle = a(\boldsymbol{u}, \boldsymbol{v}) - (\boldsymbol{f}, \boldsymbol{v}), \qquad \boldsymbol{v} \in \boldsymbol{S}^{(j)}.$$

This definition requires a suitable discrete Lagrange multiplier space $\boldsymbol{M}^{(j)}$. Here, we define the space $\boldsymbol{M}^{(j)}$ in terms of the dual Lagrange multiplier spaces introduced in [Woh00]. Let us remark, that these dual Lagrange multiplier spaces have been developed within the context of so called *mortar methods*. For structural properties as, e.g., the Ladyshenskaya Babuška Brezzi condition and discretization error estimates, see also [Woh01].

Let us now define the dual Lagrange multiplier space. Let $\lambda_p^{(j)}$ be the scalar nodal basis function associated with $p \in \mathcal{N}^{(j)} \cap \Gamma_S$. Following [Woh00, Woh01], we denote by $\psi_q^{(j)}$, $p \in \mathcal{N}^{(j)} \cap \Gamma_S$, a set of locally defined piecewise linear or bilinear biorthonormal basis functions, i.e.,

$$\int_{\Gamma_S} \psi_q^{(j)} \lambda_p^{(j)}\, dx = \delta_{qp}, \quad p, q \in \mathcal{N}^{(j)} \cap \Gamma_S\ . \tag{6.9}$$

Moreover, we assume that $P_0(\Gamma_S) \subset \text{span}\,\{\psi_q \,|\, q \in \mathcal{N}^{(j)} \cap \Gamma_S\} =: M^j$. We set

$$\boldsymbol{M}^{(j)} := (M^j)^d\,. \tag{6.10}$$

We note that in contrast to a standard mortar approach with crosspoints, no modification of the dual basis functions in the neighborhood of the endpoints of Γ_S is necessary. The discrete boundary stresses $\boldsymbol{\mu} \in \boldsymbol{M}^{(j)}$ are uniquely defined by

$$\int_{\Gamma_S} \boldsymbol{\mu}\, \boldsymbol{v}\, da = a(\boldsymbol{u}^j, \boldsymbol{v}) - f(\boldsymbol{v}), \quad \boldsymbol{v} \in \boldsymbol{S}^{(j)} \ .$$

In particular, we have $\tau = \boldsymbol{\mu} \cdot \boldsymbol{n}$, which is the desired discrete normal stress. Now, the continuous fixed point iteration (6.6) gives rise to the *discrete fixed point iteration*

$$\Psi^j \colon M_n^{(j)} \longrightarrow M_n^{(j)}\,, \qquad \tau \mapsto \Psi^j(\tau) = -\sigma_n(\boldsymbol{u}^j(\tau))\,, \tag{6.11}$$

where $\boldsymbol{u}^j$ is the unique solution of the variational inequality (6.7) and $M_n^{(j)} := \{\tau \,|\, \tau = \boldsymbol{\mu} \cdot \boldsymbol{n}\,, \boldsymbol{\mu} \in \boldsymbol{M}^{(j)}\}$. For the special choice of linear finite elements, the convergence of the discrete fixed point iteration (6.11) is shown in [LPR91]. The proof given relies on the positiveness of the shape functions for linear elements. For a detailed analysis of the discrete fixed point iteration (6.11) in case of a Lagrange multiplier space with the same structural properties as $\boldsymbol{M}^{(j)}$ we refer to [Jar83]. We remark, that the results from [Jar83, LPR91] are restricted to the case $d = 2$.

What remains is to construct a suitable modification of our monotone multigrid method for the contact problem with Tresca friction, i.e., for problem (6.7). Let us recall, that for the problem of minimizing the quadratic energy functional $\mathcal{J}$ the corresponding variational equation gives a zero of the Gâteaux–derivative of $\mathcal{J}$. Here, we cannot proceed in this way, since the functional $\hat{\mathcal{J}}$ is nondifferentiable and nonquadratic. To isolate the difficulty, let us note that the minimizer of the functional of reduced frictional energy (6.8) over $\mathcal{K}$ can equivalently be found as the minimizer of the functional

$$\hat{\mathcal{J}}(\boldsymbol{u}) = \mathcal{J}(\boldsymbol{u}) + \varphi_{\mathcal{K}}(\boldsymbol{u}) + \omega(\boldsymbol{u})\,,$$

which is defined on $\boldsymbol{H}$. Here, $\varphi_{\mathcal{K}_J}$ is the characteristic functional of the set $\mathcal{K}$. We see, that the difficulties are caused by the term $\varphi_{\mathcal{K}} + \omega$. The first term, i.e., the characteristic functional $\varphi_{\mathcal{K}}$, has already been discussed in Chapter 3. Here, we restricted the coarse grid corrections to the set of admissible displacements. Additionally, the coarse grid corrections were not allowed to cause a change of phase. In other words, we restricted the coarse grid corrections to a neighborhood of the smoothed iterate $\bar{\boldsymbol{u}}_J^\nu$ where the functional $\mathcal{J} + \varphi_{\mathcal{K}_J}$ is smooth. Following [Kor01], the same idea can be applied to piecewise smooth functionals. The functional ω is nondifferentiable and nonquadratic, but piecewise smooth. Thus, we can use *constrained Newton linearization* as proposed in [Kor01]. To this end, let us consider the smoothed iterate $\bar{\boldsymbol{u}}_J^\nu \in \boldsymbol{S}^{(J)}$ in case of Signorini's problem with Coulomb friction. Here, we additionally have to take care of the tangential displacement and the stick and slip regime. In particular to ensure convergence, the coarse grid corrections must not cause a change of phase. Thus, we define for any $p \in \mathcal{N}^{(J)\bullet}(\bar{\boldsymbol{u}}_{\boldsymbol{J}}^{\boldsymbol{\nu}})$

$$\begin{array}{lllllll}
\underline{\varphi}_J^1 &=& g(p) & , \ \overline{\varphi}_J^1 &=& \infty & , \text{ if } p \in \Gamma_S\,, \\
\underline{\varphi}_J^2 &=& (\bar{\boldsymbol{u}}_J^\nu)^2(p) & , \ \overline{\varphi}_J^2 &=& (\bar{\boldsymbol{u}}_J^\nu)^2 & , \text{ if } p \text{ is a sticky node}\,, \\
\underline{\varphi}_J^2 &=& -(\bar{\boldsymbol{u}}_J^\nu)^2(p), & \overline{\varphi}_J^2 &=& \infty & , \text{ if } p \text{ is a sliding node and } (\bar{\boldsymbol{u}}_J^\nu)^1 > 0 \\
\underline{\varphi}_J^2 &=& -\infty & , \ \overline{\varphi}_J^2 &=& -(\bar{\boldsymbol{u}}_J^\nu)^2(p), & \text{if } p \text{ is a sliding node and } (\bar{\boldsymbol{u}}_J^\nu)^1 < 0
\end{array} \ . \tag{6.12}$$

For $d = 3$, $\underline{\varphi}_J^3, \overline{\varphi}_J^3$ are defined accordingly. At all remaining nodes we set $\underline{\varphi}_J^i = -\infty$ and $\overline{\varphi}_J^i = \infty$. We now introduce the neighborhood $\mathcal{K}_{\bar{\boldsymbol{u}}_J^\nu}$ of the smoothed iterate by

$$\mathcal{K}_{\bar{\boldsymbol{u}}_J^\nu} = \{\boldsymbol{w} \in \boldsymbol{S}^{(J)} \,|\, \underline{\varphi}_J^i \leq (\bar{\boldsymbol{u}}_J^\nu)^i(p) \leq \overline{\varphi}_J^i \,\}\,.$$

We recall that the nonquadratic functional to be minimized is given by

$$\mathcal{J}(\boldsymbol{u}) + \varphi_{\mathcal{K}}(\boldsymbol{u}) + \omega_\tau(\boldsymbol{u})\,.$$

This functional is discretized by means of its $\boldsymbol{S}^{(J)}$-interpolant, i.e.,

$$\varphi_{\mathcal{K}_J}(v) + \omega^J(v) = \varphi_{\mathcal{K}_J}(v) + \sum_{p \in \mathcal{N}^{(J)} \cap \Gamma_S} \mathcal{F}\tau(p)\,|\boldsymbol{w}_T(p)|\,.$$

We discuss this discretization in detail later, see (6.16). Right now, we stick to our line of argumentation. On $\mathcal{K}_{\bar{\boldsymbol{u}}_J^\nu}$, we can linearize the smooth energy $\mathcal{J} + \omega^J_{\bar{\boldsymbol{u}}_J^\nu}$ with

$$\omega^J_{\bar{\boldsymbol{u}}_J^\nu}(\boldsymbol{w}) = \sum_{p \in \mathcal{N}^{(J)\bullet}(\bar{\boldsymbol{u}}_J^\nu)} \mathcal{F}\tau(p)\,|\boldsymbol{w}_T(p)|\,.$$

As in Chapter 3, the coarse grid corrections are restricted to a neighborhood of the smoothed iterate $\bar{\boldsymbol{u}}_J^\nu$. For contact problems without friction, the set $\mathcal{K}_{\bar{\boldsymbol{u}}_J^\nu}$ gives only rise to constraints in *normal* direction. Here, the situation is different. We also have to take into account the linearization of the functional ω^J. This leads to additional constraints in *tangential* direction, see (6.12). The extended relaxation steps (3.2) are now done with respect to the quadratic energy functional $\hat{\mathcal{J}}_{\bar{\boldsymbol{u}}_J^\nu}$, which is given by

$$\hat{\mathcal{J}}_{\bar{\boldsymbol{u}}_J^\nu}(\boldsymbol{w}) = \frac{1}{2} a(\boldsymbol{w}, \boldsymbol{w})_{\bar{\boldsymbol{u}}_J^\nu} - f(\boldsymbol{w})_{\bar{\boldsymbol{u}}_J^\nu}$$

with

$$a(\boldsymbol{w}, \boldsymbol{w})_{\bar{\boldsymbol{u}}_J^\nu} = a(\boldsymbol{w}, \boldsymbol{w}) + \omega''_{\bar{\boldsymbol{u}}_J^\nu}(\bar{\boldsymbol{u}}_J^\nu)(\boldsymbol{w}, \boldsymbol{w})$$

and

$$f(\boldsymbol{w})_{\bar{\boldsymbol{u}}_J^\nu} = f(\boldsymbol{w}) - \omega'_{\bar{\boldsymbol{u}}_J^\nu}(\bar{\boldsymbol{u}}_J^\nu)(\boldsymbol{w}) + \omega''_{\bar{\boldsymbol{u}}_J^\nu}(\bar{\boldsymbol{u}}_J^\nu)(\bar{\boldsymbol{u}}_J^\nu, \boldsymbol{w})\,,$$

respectively. In particular, the resulting *quadratic* obstacle problem: Find $\boldsymbol{w} \in \mathcal{K}_{\bar{\boldsymbol{u}}_J^\nu}$, such that

$$\hat{\mathcal{J}}_{\bar{\boldsymbol{u}}_J^\nu}(\boldsymbol{w}) \leq \hat{\mathcal{J}}_{\bar{\boldsymbol{u}}_J^\nu}(\boldsymbol{v})\,, \qquad \boldsymbol{v} \in \mathcal{K}_{\bar{\boldsymbol{u}}_J^\nu}\,.$$

gives rise to a *constrained Newton linearization*. For a detailed analysis, see [Kor01]. In consequence, we do not only have to take the constraints in normal direction into account but also the constraints in tangential direction. Moreover in each step of our monotone multigrid method, we have to modify the coarse grid stiffness matrices with respect to $\omega''_{\bar{\boldsymbol{u}}_J^\nu}(\bar{\boldsymbol{u}}_J^\nu)$.

We consider the local nonlinear subproblems which have to be solved in the leading relaxation. The local corrections $\boldsymbol{v}_l$ from (3.2) are the unique solutions of the local subproblems: Find $\boldsymbol{v}_l \in \boldsymbol{V}_l$ such that

$$\hat{\mathcal{J}}(\boldsymbol{w}_{l-1} + \boldsymbol{v}_l) \leq \hat{\mathcal{J}}(\boldsymbol{w}_{l-1} + \boldsymbol{v}), \qquad \boldsymbol{v} \in \boldsymbol{V}_l. \tag{6.13}$$

Using (6.16), this can be equivalently rewritten as the following variational inclusion: Find $\boldsymbol{v}_l \in \boldsymbol{V}_l$, such that

$$0 \in a(\boldsymbol{v}_l, \boldsymbol{v}) - (f(\boldsymbol{v}_l) - a(\boldsymbol{w}_{l-1}, \boldsymbol{v})) + \partial(\varphi_{\mathcal{K}_J} + \omega_\tau^J)(\boldsymbol{w}_{l-1} + \boldsymbol{v}_l)(\boldsymbol{v}), \qquad \boldsymbol{v} \in \boldsymbol{V}_l, \tag{6.14}$$

where ∂ denotes the subdifferential as introduced in (2.20). The variational inclusion (6.14) gives rise to a local nonlinear system. In a next step, we consider this nonlinear system in more detail. Let p_l be the node associated with $\boldsymbol{V}_l$. We set

$$r_{p_l}^i = f(\lambda_{p_l}^{(J)} \boldsymbol{e}_{p_l}^i) - a(\boldsymbol{w}_{l-1}, \lambda_{p_l}^{(J)} \boldsymbol{e}_{p_l}^i), \qquad a_{p_l p_l}^{ij} = a(\lambda_{p_l}^{(J)} \boldsymbol{e}_{p_l}^i, \lambda_{p_l}^{(J)} \boldsymbol{e}_{p_l}^j).$$

and we have $(r_{p_l}^i)_{1 \leq i \leq d} = \boldsymbol{r}_{p_l} \in \mathbb{R}^d$ and $(a_{p_l p_l}^{ij})_{1 \leq i,j \leq d} = \boldsymbol{a}_{p_l p_l} \in \mathbb{R}^{d \times d}$. We remark, that $\boldsymbol{a}_{p_l p_l}$ is a diagonal $d \times d$ block matrix entry of the stiffness matrix on level J. Using these definitions, the variational inclusion (6.14) can equivalently be rewritten as the inclusion: Find $\bar{\boldsymbol{z}}_{p_l} \in \mathbb{R}^d$ such that

$$\boldsymbol{0} \in \boldsymbol{a}_{p_l p_l} \bar{\boldsymbol{z}}_{p_l} - \boldsymbol{r}_{p_l} + \partial \Phi_{p_l}(\bar{\boldsymbol{z}}_{p_l}). \tag{6.15}$$

Here, Φ_{p_l} is a suitable subdifferentiable functional.We define Φ_{p_l} in terms of a discretization of the reduced frictional functional ω_τ and the characteristic functional $\varphi_{\mathcal{K}}$. The discretization of the reduced frictional functional ω_τ is realized by means of its $\boldsymbol{S}^{(J)}$-interpolant and the dual basis functions $\psi_q^{(J)}$. We define the function $\Phi^T \colon \mathbb{R}^{d-1} \longrightarrow \mathbb{R}$ by $\Phi^T(\boldsymbol{v}_T) = |\boldsymbol{v}_T|$ and set

$$\begin{aligned} \omega_\tau^J(\boldsymbol{v}) &= \int_{\Gamma_S} \sum_{p,q \in \mathcal{N}^{(J)} \cap \Gamma_S} \mathcal{F}\tau(q) \psi_q^{(J)} \, \Phi^T(\boldsymbol{v}_T(p)) \, \lambda_p^{(J)} \, dx & (6.16) \\ &= \sum_{p \in \mathcal{N}^{(J)} \cap \Gamma_S} \mathcal{F}\tau(p) \, \Phi^T(\boldsymbol{v}_T(p)). & (6.17) \end{aligned}$$

Here, we have exploited the property (6.9) of the dual basis functions $\psi_q^{(J)}$. To define the discretization of the characteristic functional, we introduce $\Phi^{n,p} \colon \operatorname{dom} \Phi^{n,p} \subset \mathbb{R} \longrightarrow \mathbb{R}$ by

$$\Phi^{n,p}(z_n) = \begin{cases} +\infty & , \quad z_n > g(p) \\ 0 & , \quad z_n \leq g(p) \end{cases},$$

$z_n \in \mathbb{R}$. Now, the discretization of $\varphi_{\mathcal{K}}$ is given by

$$\varphi_{\mathcal{K}_J}^J(\boldsymbol{v}) = \sum_{p \in \mathcal{N}^{(J)} \cap \Gamma_S} \Phi^{n,p}(v_n(p)).$$

As is done in [Kor97a] for the scalar case, we define the convex function Φ_{p_l} by

$$\Phi_{p_l}(\boldsymbol{z}) = \varphi_{\mathcal{K}_J}^J(\boldsymbol{w}_{l-1} + z^i \boldsymbol{e}^i(p_l)) + \omega_\tau^J(\boldsymbol{w}_{l-1} + z^i \boldsymbol{e}^i(p_l)), \qquad \boldsymbol{z} \in \mathbb{R}^d.$$

The subdifferential $\partial\Phi_{p_l}(\boldsymbol{z})$ of Φ_{p_l} is given by

$$\partial\Phi_{p_l}(\boldsymbol{z}) = \partial\Phi(\boldsymbol{w}_{l-1}(p_l) + \boldsymbol{z})\,, \qquad \boldsymbol{z} \in \text{dom } \partial\Phi_{p_l}\,.$$

To obtain a solution of the inclusion (6.15), we have to compute the subdifferential of the function Φ. This is done in the following lemma.

Lemma 6.5 *Let $z_n \in \mathbb{R}$. The subdifferential of the scalar convex function $\Phi^{n,p}$ is given by*

$$\partial\Phi^{n,p}(z_n) = \begin{cases} 0 & , \quad z_n < g(p) \\ [0,\infty) & , \quad z_n = g(p) \end{cases},$$

with $z_n \in \mathbb{R}$. Let $\boldsymbol{z}_T \in \mathbb{R}^{d-1}$. The subdifferential of the convex function Φ^T is given by

$$\partial\Phi^T(\boldsymbol{z}_T) = \begin{cases} \{\boldsymbol{\mu}\,|\;\; |\boldsymbol{\mu}| \le 1\} & , \quad \boldsymbol{z}_T = 0\,, \\ \boldsymbol{z}_T/|\boldsymbol{z}_T| & , \quad \boldsymbol{z}_T \neq 0\,, \end{cases},$$

with $\boldsymbol{\mu} \in \mathbb{R}^{d-1}$.

Proof Let $z_n' \in \mathbb{R}$ and let $\mu \in \mathbb{R}$. Then from the definition of the subdifferential (2.20), we get for all z_n, $z_n' < g(p)$

$$\Phi^{n,p}(z_n') - \Phi^{n,p}(z_n) = 0 \ge \mu \cdot (z_n' - z_n)$$

and thus $\mu = 0$. For the case $z_n = g(p)$, $z_n' < g(p)$ we have $z_n' - z_n < 0$ and thus

$$\Phi^{n,p}(z_n') - \Phi^{n,p}(z_n) = 0 \ge \mu \cdot (z_n' - z_n)$$

for all $\mu \ge 0$. Since $\Phi^{n,p}(z_n') = +\infty$ for $z_n' >$ g(p), the assertion follows. To proof the second assertion, it suffices to consider the case $\boldsymbol{z}_T = 0$. In this case, we have for $\mu, \boldsymbol{z}_T' \in \mathbb{R}^{d-1}$

$$\Phi^T(\boldsymbol{z}_T') - \Phi^T(\boldsymbol{z}_T) = |\boldsymbol{z}_T'| \ge |\boldsymbol{\mu}| \cdot |\boldsymbol{z}_T'| \ge (\boldsymbol{\mu}, \boldsymbol{z}_T')\,,$$

if $|\boldsymbol{\mu}| \le 1$.

□

Let us assume, there is no contact at p_l. Then, we find $\tau(p_l) = 0$ and thus $\mathbf{0} = \boldsymbol{a}_{p_l p_l}\boldsymbol{u}_{p_l} - \boldsymbol{r}_{p_l}$. Here, we have introduced the unknown correction $\boldsymbol{u}_{p_l} = u^i_{p_l}\boldsymbol{e}^i(p_l) \in \mathbb{R}^d$ given with respect to the rotated coordinate system $\{\boldsymbol{e}^i(p_l)\}$ with $\boldsymbol{e}^1(p_l) = \boldsymbol{n}(p_l)$. It remains to consider the case of contact at p_l. Then, there are two possibilities. Either, p_l is a sticky node, and we have $\boldsymbol{u}_{p_l} = (g(p_l), \mathbf{0})^T$ or p_l is a sliding node and we have $\boldsymbol{u}_{p_l} = (g(p_l), \boldsymbol{v}_T)^T$ with $\boldsymbol{v}_T \neq 0$. We note that using the *modified residual* $\tilde{\boldsymbol{r}}_{p_l} = \boldsymbol{r}_{p_l} + \boldsymbol{a}_{p_l p_l}\boldsymbol{w}_{l-1}(p_l)$ and setting $\boldsymbol{u}_{p_l} = \boldsymbol{w}_{l-1}(p) + \bar{\boldsymbol{z}}$, we see that the inclusion (6.15) can be written as

$$\mathbf{0} \in \boldsymbol{a}_{p_l p_l}\boldsymbol{u}_{p_l} - \tilde{\boldsymbol{r}}_{p_l} + \partial\Phi(\boldsymbol{u}_{p_l})\,.$$

Let now $\tilde{\boldsymbol{u}}_{p_l} = (g(p_l), \mathbf{0})^T$ and let

$$\sigma_T(\tilde{\boldsymbol{u}}_{p_l}) = (\boldsymbol{a}_{p_l p_l}\tilde{\boldsymbol{u}}_{p_l} - \tilde{\boldsymbol{r}}_{p_l})_T \,.$$

Let us first consider the case $|\sigma_T(\tilde{\boldsymbol{u}}_{p_l})| \leq \mathcal{F}\tau(p_l)$. Then p_l is a sticky node, since the solution of the variational inclusion (6.14) is unique. In the second case, we have to solve the local nonlinear system

$$\boldsymbol{a}_{p_l p_l}\boldsymbol{u}_{p_l} - \tilde{\boldsymbol{r}}_{p_l} = -\begin{pmatrix} \mu \\ \mathcal{F}\cdot\tau\,\boldsymbol{u}_T/|\boldsymbol{u}_T| \end{pmatrix}, \tag{6.18}$$

for $0 \leq \mu \in \mathbb{R}$. We remark that the value of μ is unknown and the value for u_n is known, $u_n = u^1 = g(p_l)$. The unknowns in (6.18) are $\boldsymbol{u}_T$ and μ. In two space dimensions, $u_T/|u_T| \in \{-1, 1\}$ and thus (6.18) can easily be solved. More precisely, at most two linear twodimensional system, have to be solved. The situation is completely different for problems in three space dimensions. Here, the boundary of the unit sphere is a onedimensional curve. We solve the arising local subproblems iteratively using a Uzawa method, see [Glo84, p. 170].

Remark 6.6 *If the tangential displacement of a sliding node is very small, even a damped Newton method fails to solve the local subproblems in three space dimensions. This problem does not arise in two space dimensions, since here the boundary of the unit sphere consists of only two points.*

Now, we can give our first algorithm for solving Signorini's problem with Coulomb friction.

Algorithm 2 (Jacobi like fixed point iteration)

Initialize: $\boldsymbol{u}_0^0 = \mathbf{0}$, $\tau_0^0 = 0$
Level: for $j = 0, \ldots, J$ do
Initialize: Assemble stiffness matrix $\boldsymbol{A}$ and right hand side $\boldsymbol{f}$
Normal stress: for $k = 1, \ldots, K$ do
Solve nonlinear contact problem with Tresca Friction and given normal stress
Find $\boldsymbol{u}_j^k \in \mathcal{K}_j$ by applying sufficiently many multigrid steps to

$$(\boldsymbol{A}\boldsymbol{u}_j^k, \boldsymbol{v} - \boldsymbol{u}_j^k) + \boldsymbol{\omega}^j_{\tau_j^{k-1}}(\boldsymbol{u}_j^k) - \boldsymbol{\omega}^j_{\tau_j^{k-1}}(\boldsymbol{v}) \quad \geq \quad (\boldsymbol{f}, \boldsymbol{v} - \boldsymbol{u}_j^k), \qquad \boldsymbol{v} \in \boldsymbol{S}^{(j)} \,.$$

Compute the boundary stress $\boldsymbol{\mu}_j^k \in \boldsymbol{S}^{(j)}$: $\boldsymbol{\mu}_j^k = \boldsymbol{A}\boldsymbol{u}_j^k - \boldsymbol{f}$.
Compute normal stress: $\tau_j^k = \mu_n$
Estimate error and refine
Interpolate solution: $\boldsymbol{u}_{j+1}^0 = \mathcal{I}_{j-1}^j \boldsymbol{u}_j^K$
Interpolate normal stress: $\boldsymbol{\tau}_{j+1}^0 = (\mathcal{I}_{j-1}^j \boldsymbol{\mu}_j^K)_n$

Here, $\boldsymbol{\omega}_{\cdot}^{j}(\cdot)$ denotes the algebraic representation of the functional $\omega_{\cdot}^{j}(\cdot)$. It is also possible to stop the outer iteration in the boundary stresses if some suitable stopping criterion is satisfied, e.g.,

$$\frac{\|\tau_j^{k+1} - \tau_j^k\|}{\|\tau_j^{k+1}\|} \leq \varepsilon$$

for some prescribed tolerance ε. Here, $\|\cdot\|$ stands for the Euclidian vector norm.

In what follows, we present a new algorithm for solving contact problems with friction. In Algorithm 2, the normal stress is updated after the reduced frictional problem has been solved. It is also possible to update the prescribed discrete normal stress τ after *each* intermediate iteration step. In the resulting monotone multigrid method, we use all information on the nonlinearity as soon as it is available. Thus, we expect much faster convergence than from Algorithm 2. We replace the local subproblems (6.13) in the leading Gauß–Seidel iteration by the local subproblems

$$\boldsymbol{v}_l \in \boldsymbol{V}_l : \quad \tilde{\mathcal{J}}_{\boldsymbol{w}_{l-1}}(\boldsymbol{w}_{l-1} + \boldsymbol{v}_l) \leq \tilde{\mathcal{J}}_{\boldsymbol{w}_{l-1}}(\boldsymbol{w}_{l-1} + \boldsymbol{v}), \qquad \boldsymbol{v} \in \boldsymbol{V}_l . \tag{6.19}$$

Here, the functional $\tilde{\mathcal{J}}_{\boldsymbol{w}}$ is defined by

$$\tilde{\mathcal{J}}_{\boldsymbol{w}} = \mathcal{J} + \varphi_{\mathcal{K}} + \omega_{|\sigma_n(\boldsymbol{w})|} = \mathcal{J} + \varphi_{\mathcal{K}} + \omega(\boldsymbol{w}, \cdot) .$$

Unfortunately, the functional $\tilde{\mathcal{J}}_{(\cdot)}(\cdot)$ is nonconvex. No proof of convergence of the successive minimization induced by (6.19) is known. Let us now state our Gauß–Seidel like algorithm.

Algorithm 3 (Gauß–Seidel like iteration)

Initialize: $\boldsymbol{u}_0^0 = \boldsymbol{0}$
Level: for $j = 0, \ldots, J$ do
Initialize: Assemble stiffness matrix $\boldsymbol{A}$ and right hand side $\boldsymbol{f}$
Set $\boldsymbol{w}_j^0 = \boldsymbol{0}$.
Solve nonlinear contact problem with friction:
Find $\boldsymbol{u}_j^k \in \mathcal{K}_j$ by carrying out sufficiently many of the following multigrid steps:
For $l = 1, \ldots, n_j$ do
Compute local corrections $\boldsymbol{v}_j^l \in \boldsymbol{V}_l$ according to

$$(\boldsymbol{A}\boldsymbol{v}_j^l, \boldsymbol{v} - \boldsymbol{v}_j^l) + \boldsymbol{\omega}^j(\boldsymbol{w}_j^{l-1}, \boldsymbol{v}) - \boldsymbol{\omega}^j(\boldsymbol{w}_j^{l-1}, \boldsymbol{v}_j^l) \quad \geq \quad (\boldsymbol{f}, \boldsymbol{v} - \boldsymbol{v}_j^l), \qquad \boldsymbol{v} \in \boldsymbol{V}_l .$$

Update of the intermediate iterate: $\boldsymbol{w}_j^l = \boldsymbol{w}_j^{l-1} + \boldsymbol{v}_j^l$
Compute smoothed iterate: $\bar{\boldsymbol{u}}_j = \boldsymbol{w}_j^{n_j}$
Compute coarse grid correction $\boldsymbol{c}$ with respect to $\hat{J}_{\bar{\boldsymbol{u}}_j}$
Set $\boldsymbol{u}_j = \bar{\boldsymbol{u}}_j + c$
Interpolate solution: $\boldsymbol{u}_{j+1}^0 = \mathcal{I}_{j-1}^j \boldsymbol{u}_j$

We note that the extended relaxation steps are the same for Algorithm 2 and 3. The advantage of Algorithm 3 is that *no outer iteration in the normal stress is required.* We point out that the inner iteration in Algorithm 3 is a local iteration, whereas the inner iteration of Algorithm 2 requires the solution of a global contact problem with given friction. However, the question of convergence of Algorithm 3 is open. This is in contrast to the discrete fixed point iteration (6.11). Nevertheless, to our knowledge there are no results concerning the convergence *speed* of (6.11). In our numerical experiments, we observe rapid convergence of (6.11). Also in all of our numerical experiments, Algorithm 3 converges significantly faster than Algorithm 2. Both algorithms give asymptotically the same results. For a more detailed analysis we refer to the next section.

The differences between Algorithms 2 and 3 can also be interpreted as follows: In Algorithm 2, the normal stress is associated with the outer iteration, whereas in Algorithm 3 it is associated with the local relaxation. In Algorithm 2, we have to apply in each iteration step our multigrid method, whereas in Algorithm 3 only one multigrid solver has to be applied.

6.3 Numerical Results

In this section, we present numerical results illustrating the performance of Algorithm 2 and Algorithm 3 for Signorini's problem with Coulomb friction. In our numerical experiments, Algorithm 2 as well as Algorithm 3 turn out to be a reliable tool for solving frictional contact problems. In particular, the fixed point iteration shows to converge rapidly. Using nested iteration, we also observe the necessary number of fixed point iterations to be bounded independent of the level. Thus using monotone multigrid method as an inner solver, the computational effort for solving a nonlinear contact problem with friction is proportional to the number of unknowns. Using the Gauß–Seidel like Algorithm 3 instead of Algorithm 2, even no outer iteration is necessary.

In the rest of this section we proceed as follows. We start with a twodimensional example and followed by a threedimensional example. In both examples, we compare Algorithm 2 and Algorithm 3. For results concerning the elastic contact of two bodies with friction, we refer the reader to Section 7.2. For both of the following examples, we use sufficiently many steps of a $\mathcal{W}(3,3)$-cycle of our monotone multigrid method as inner solver. In three space dimensions, we apply truncation in normal and tangential direction at a node p, if contact at p has been found. Proceeding in this way does not slow down the convergence significantly, but reduces the computational effort needed for the reassembling of the coarse grid matrices.

We start with the Hertzian contact problem described in Section 5.1. In contrast to Section 5.1, we enforce Coulomb friction at Γ_S with coefficient of friction $\mathcal{F} = 0.4$. Moreover, adaptive refinement is controlled by a residual based error indicator and not by the hierarchical error estimator used in Section 5.1. The discrete solution on the final Level $J = 10$ is obtained using Algorithm 2. Since our aim is to study the quantitative aspects of the fixed point iteration, we stop the inner iteration on each level j if

$$\frac{\|\boldsymbol{u}_j^{k+1} - \boldsymbol{u}_j^k\|}{\|\boldsymbol{u}_j^{k+1}\|} \leq 10^{-9}\,.$$

The fixed point iteration, i.e., the outer iteration, is stopped on each level j, if the stopping criterion

$$\varepsilon_j^k := \frac{\|\tau_j^{k+1} - \tau_j^k\|}{\|\tau_j^{k+1}\|_2} \leq 2 \cdot 10^{-7}$$

is satisfied. The number of necessary outer iterations is shown in Table 6.1. As an estimate for the convergence speed of the outer iteration, we define the average estimated convergence rate of the fixed point iteration

$$\rho_\tau^j := \left(\prod_{k=1}^{K} \varepsilon_j^k \right)^{1/K} .$$

The estimated convergence rate is given in the last column of Table 6.1. The values printed in the last column are also shown in the left picture of Figure 6.5. As it can be seen, the number of outer iterations does not increase with the refinement level. Moreover, the fixed point iteration converges rapidly. We also applied Algorithm 3 to the Hertzian contact

Level	dof	# contact	# sticky	# outer it.	# Jac	#GS	ρ_τ^j
0	94	—	—	— 1	—	—	—
1	330	1	1	1	12	12	—
2	1 234	3	1	3	32	14	$1.9 \cdot 10^{-4}$
3	1 602	5	3	4	32	9	$2.3 \cdot 10^{-3}$
4	2 200	7	3	5	39	9	$1.9 \cdot 10^{-2}$
5	3 274	15	7	6	45	11	$4.4 \cdot 10^{-2}$
6	5 330	29	13	7	46	10	$6.0 \cdot 10^{-2}$
7	9 114	57	27	7	45	13	$6.1 \cdot 10^{-2}$
8	1 6646	113	53	7	45	11	$6.1 \cdot 10^{-2}$
9	31 596	225	107	7	45	17	$6.0 \cdot 10^{-2}$
10	64 870	449	213	7	45	13	$6.0 \cdot 10^{-2}$

Table 6.1: Performance of the fixed point iteration, twodimensional example

problem. In the column entitled "# Jac" the total number of $\mathcal{W}$-cycles for Algorithm 2 is printed, in the column entitled "# GS" the total number of $\mathcal{W}$-cycles for Algorithm 3 is printed. As it turns out, Algorithm 3 and Algorithm 2 give asymptotically the same results, but Algorithm 3 does not require an outer iteration in the normal stresses. Moreover, for this example it is about *four times faster* than Algorithm 2. Since the nonlinearity is resolved within the multigrid cycle by solving local nonlinear problems, the optimal complexity of one iteration step is preserved. In particular, the computational cost of solving a nonlinear contact problem with friction is comparable to the cost of solving a *linear* problem.

The resulting boundary stresses are shown in the middle of Figure 6.4. Between the two "peaks" of the tangential stresses, we have the sticky region. Here, the tangential stresses increase until the critical stress $\mathcal{F}|\boldsymbol{u}_n|$ is reached. Then, sliding occurs and the

tangential stresses decrease. We emphasize that by construction our method separates sticky and slippy nodes, i.e., we do not only compute the displacements but get also the phase of each node in Γ_S for free. To illustrate the effect of different coefficients of Friction, in Figure 6.4 the boundary stresses for $\mathcal{F} = 0.05, 0.4, 1.0$ are depicted. In the case $\mathcal{F} = 0.05$, there is only one sticky node on the final level, all other nodes are sliding nodes. In the case $\mathcal{F} = 1.0$, for the sliding nodes we expect the tangential stresses to coincide with the normal stresses. This behavior is perfectly shown by our discrete approximation.

For different twodimensional numerical examples, the performance of the fixed point iteration (6.11) is also investigated in [LPR91]. A successive over relaxation method is used as the inner solver. The authors observe a constant number of outer iterations on each refinement level for small coefficients of Friction $\mathcal{F}$. For large coefficients of Friction, i.e., $5 \leq \mathcal{F} \leq 100$, they observe convergence depending on the chosen grid. These results are in good agreement with the results of our numerical experiments. For a different to the solution of contact problems with friction, see, e.g., [PC99, DV97] and [RCL88] for a survey. Our next example is the elastic cylinder on two rigid rods as presented in Section

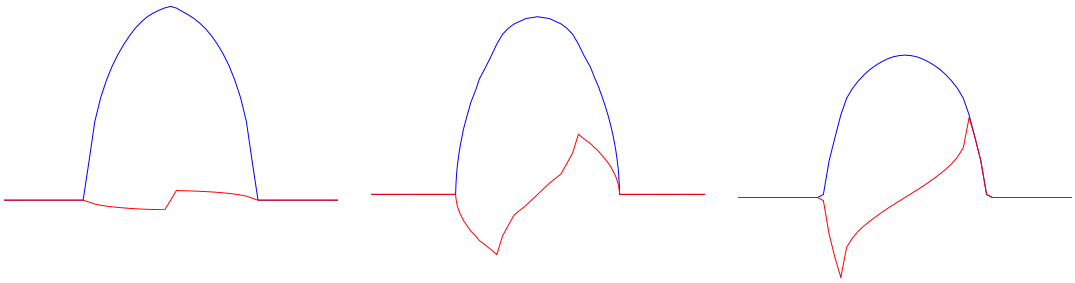

Figure 6.4: Normal stress (blue) and tangential stress (red) for the Hertzian contact problem with $\mathcal{F} = 0.05, 0.4, 1.0$

5.3. In contrast to Section, 5.3 here we use a coarse grid with only one element. Moreover we use adaptive refinement, controlled by a residual based error indicator. We solve Signorini's problem with Coulomb friction using Algorithm 2 and Algorithm 3. In Table 6.2, the number of outer iterations on each level is shown. As in the twodimensional example, we also give the numbers ρ_τ^j in the last column. The significant increase of the number of inner iterations is caused by degenerating elements near the boundary of the cylinder. Due to the extremely coarse initial grid, the shape regularity is lost when approximating the curved boundary on finer grids. This is in contrast to Section 5.3, where we have used a different coarse grid. However, this does not affect the outer iteration. Again, the fixed point iteration shows to converge rapidly. We also applied Algorithm 3 to this example. As before, in the column entitled "# Jac" the total number of $\mathcal{W}$-cycles for Algorithm 2 is printed and in the column entitled "# GS" the total number of $\mathcal{W}$-cycles for Algorithm 3 is printed. Asymptotically, Algorithm 3 yields the same results as Algorithm 2. For this example, Algorithm 3 is about *four times faster* than Algorithm 2. Compared to the case of two space dimensions, the computational cost of one multigrid cycle is considerably higher. Thus especially in three dimensions, it is important to have an

Level	dof	# contact	# sticky	# outer it.	# Jac	# GS	ρ_τ^j
0	27	—	—	—	—	—	—
1	567	6	2	5	72	23	$4.1 \cdot 10^{-2}$
2	3 723	14	4	4	63	17	$2.2 \cdot 10^{-2}$
3	10 194	46	18	5	75	18	$2.2 \cdot 10^{-2}$
4	37 935	180	56	5	87	21	$4.3 \cdot 10^{-2}$
5	92 961	684	188	6	146	32	$5.9 \cdot 10^{-2}$
6	226 500	2 728	747	6	274	70	$7.2 \cdot 10^{-2}$

Table 6.2: Performance of the fixed point iteration, threedimensional example

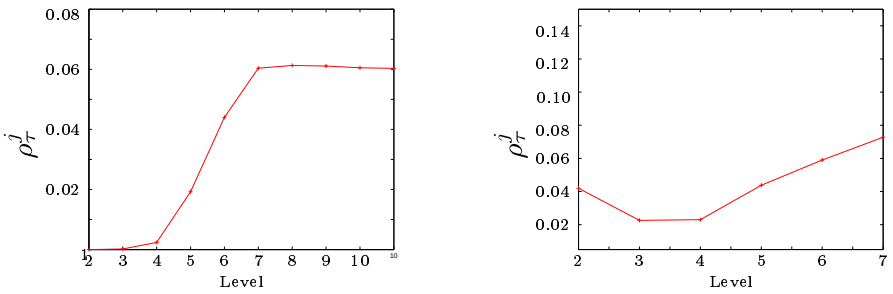

Figure 6.5: Performance of the discrete fixed point iteration, Hertzian example (left) and cylinder (right)

iteration scheme without outer iteration. This is provided by Algorithm 3. The numbers ρ_τ^j are depicted in the right picture of Figure 6.5. In Figure 6.6, the tangential stresses

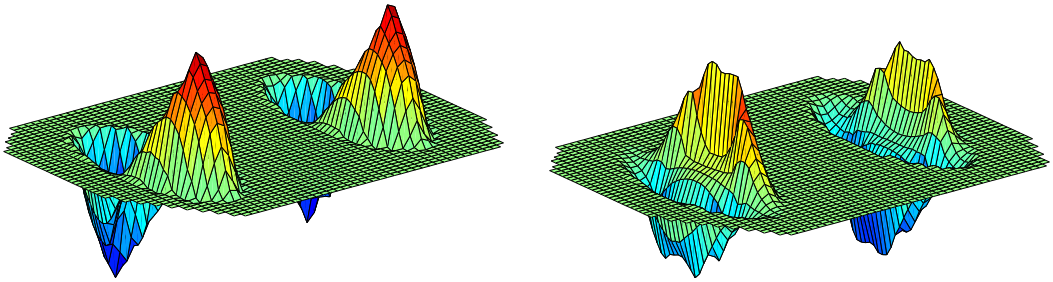

Figure 6.6: Tangential stresses for the three dimensional cylinder example

with respect to the local coordinate systems $\{\boldsymbol{e}_i(p)\}$, $\boldsymbol{e}_1(p) = \boldsymbol{n}(p)$ and $p \in \mathcal{N}^{(5)} \cap \Gamma_S$ are depicted. Note that the tangential stresses show a similar structure as for the Hertzian contact problem.

Remark 6.7 *In our implementation, the modification of the coarse grid matrices due to the additional linearization terms is done locally as described in Section 4.5. We also performed numerical experiments in three space dimension, where we omitted the additional linearization terms. Here, for some problems the convergence of the method was lost due to wrong coarse grid corrections. For two dimensional problems no additional terms are necessary at all, because in this case $|v_T|$ is piecewise linear..*

It is also possible to truncate any node being in contact with the foundation in normal and *tangential direction, regardless of it being a sticky or slippy node. In this case, the stiffness matrices on the coarser grids remain unaltered.*